

Research Article

Travelling Wave Analysis of a Diffusive COVID-19 Model

C. M. Wachira ¹, G. O. Lawi ¹ and L. O. Omondi ²

¹Department of Mathematics, Masinde Muliro University of Science and Technology, Kenya

²Department of Mathematics, Egerton University, Kenya

Correspondence should be addressed to G. O. Lawi; glawi@mmust.ac.ke

Received 19 July 2022; Accepted 16 September 2022; Published 7 October 2022

Academic Editor: Tudor Barbu

Copyright © 2022 C. M. Wachira et al. This is an open access article distributed under the Creative Commons Attribution License, which permits unrestricted use, distribution, and reproduction in any medium, provided the original work is properly cited.

In this paper, a mathematical model based on a system of nonlinear parabolic partial differential equations is developed to investigate the effect of human mobility on the dynamics of coronavirus 2019 (COVID-19) disease. Positivity and boundedness of the model solutions are shown. The existence of the disease-free, the endemic equilibria, and the travelling wave solutions of the model are shown. From the numerical analysis, it is shown that human mobility plays a crucial role in the disease transmission. Therefore, interventions that affect diffusion (human mobility), such as lock-down, travel restrictions, and cessation of movement, may play a significant role in controlling and preventing the spread of COVID-19.

1. Introduction

COVID-19 disease, caused by SARS-COV-2 virus emerged from the city of Wuhan, Hubei Province, China in late December 2019 and quickly spread all over the world [1]. This global spread was greatly facilitated by movement of infectious individuals from Wuhan city (the epicenter) to other parts of the world where there were no COVID-19 infections. The disease was declared a global health pandemic by the World Health Organization (WHO) on 11th of March, 2020. The virus is primarily transmitted to humans through inhaling respiratory droplets produced by sneezing, coughing, and conversing with an infectious person (direct transmission) or indirectly through contact with contaminated surfaces (indirect transmission) [2]. COVID-19 incubation period, which is the time between virus exposure and symptom onset, is on average 5–6 days, but can be as long as 14 days [3]. Fever, a dry cough, and fatigue are the most common symptoms of COVID-19. Body aches and pains, a sore throat, diarrhoea, headache, loss of taste and smell, breathing difficulties, a rash on the skin, and discoloration of the fingers and toes are some of the other symptoms [1, 2].

There were no antiviral prophylaxis or therapeutics available during the early phases of the COVID-19 outbreak, so all affected countries relied on nonpharmaceutical inter-

ventions such as isolation and quarantine of infected individuals, contact tracing, and population lockdown [4]. These interventions are aimed at containing and mitigating the epidemic, that was a threat to many health-care systems. These preventive measures appeared to be effective in lowering the number of fatalities and hospitalizations [4, 5]. COVID-19 vaccine candidates have been developed and are already in use [6]. Vaccines such as BNT162b2 (Pfizer), mRNA1273 (Moderna), ChAd0x1 nCoV-19 (Astra Zeneca), Sputnik, Sinopharm, and Johnson & Johnson vaccines are currently being administered worldwide.

The dynamics of COVID-19 pandemic have been complex in both time and space. These dynamics are caused by a number of factors, including the spatial distribution of the population's social and economic levels and the patterns of human mobility within a given country [7]. Human mobility may be due to travel, migration between localities, countries, or towns. When infected people travel to infection-free areas, there is a good risk that they will pass their infections on to locals. The transfer of infections from a region of high concentration to a region of low concentration causes a wave of transfer of infection.

A variety of mathematical models have been used widely in various biological applications such as ecology, population dynamics, tumor growth (cancer), immunology, and epidemiology [8, 9]. A number of epidemics have been

modeled using reaction-diffusion equations with the focus to demonstrate the existence of travelling wave solutions in work such as in references [10, 11]. Reaction-diffusion epidemic models are generally standard epidemic models that assume there is movement and interaction of individuals in a given population in space.

Human mobility restrictions such as lock-down, travel restrictions, and cessation of movement are regarded as an effective strategy for controlling disease spread. However, it is still unclear whether mobility restriction is a proportional response to control the ongoing COVID-19 pandemic [12]. In this paper, the existence of travelling wave solutions as well as the effect of human mobility (diffusion) on the transmission dynamics of COVID-19 disease are investigated.

2. Model Formulation

In this study the transmission dynamics of COVID-19 is assumed to be determined by the spatial location, x , as well as time, t . Despite the fact that the underlying conditions mentioned in the previous section predisposes someone to a higher risk of contracting COVID-19 disease, because the focus is on human mobility, the study assumes the differential susceptibility. Individuals in this category are referred to as susceptible individuals, which are denoted by the symbol $S(x, t)$. When susceptible individuals are exposed to the virus, they undergo an incubation period, which is the time between virus exposure and onset of symptoms. This is on average 5–6 days, but can be as long as 14 days [3]. The incubating individuals here are categorised as the exposed class, denoted by $E(x, t)$. Following the end of the exposure period, the incubating individuals transit into the infection class denoted by $I(x, t)$. The infectious potential of COVID-19 is significantly greater just before or within the first five days of symptom onset [13]. Therefore, the infected class $I(x, t)$ in this study will include both individuals with and without symptoms. Depending on the severity of symptoms and the intervention strategies in place, the infected individuals may die or recover from the disease. Thus, the class $R(x, t)$ denotes the number of individual who have recovered from the infection.

It is assumed that susceptible humans are recruited at a constant rate Λ . The susceptible humans become infected through a force of infection $((\beta SI)/(1 + \eta I))$, where β is the transmission coefficient, and η is the half-maximal human saturation constant of the infected individuals. It is considered to be of Michaelis–Menten form to account for saturation of the human infection [14]. The saturated incidence given by $((\beta SI)/(1 + \eta I))$ is reasonable due to the fact that as the infected individuals increase, they reach a saturation point. The number of infected individuals decreases due to psychological effects, behavioral changes, or preventive measures taken by the affected individuals [15]. The rate of progression from the exposed to infected classes is assumed to be ε . The rates of natural and disease-induced mortality are μ and δ , respectively. The recovery rate from the infection is taken as λ . The diffusivity of susceptible, exposed, infected, and recovered individuals are d_1, d_2, d_3 , and d_4 , respectively.

The corresponding proposed mathematical equations arising from the preceding description can be described by the following system of partial differential equations:

$$\frac{\partial S}{\partial t} - d_1 \nabla^2 S = \Lambda - \frac{\beta SI}{1 + \eta I} - \mu S, \quad (1)$$

$$\frac{\partial E}{\partial t} - d_2 \nabla^2 E = \frac{\beta SI}{1 + \eta I} - (\mu + \varepsilon)E, \quad (2)$$

$$\frac{\partial E}{\partial t} - d_2 \nabla^2 E = \frac{\beta SI}{1 + \eta I} - (\mu + \varepsilon)E, \quad (3)$$

$$\frac{\partial I}{\partial t} - d_3 \nabla^2 I = \varepsilon E - (\mu + \lambda + \delta)I, \quad (4)$$

$$\frac{\partial R}{\partial t} - d_4 \nabla^2 R = \lambda I - \mu R, \quad (5)$$

where $\{S(x, t), E(x, t), I(x, t), R(x, t)\} \in \Psi \times T \subset \mathbb{R}_+^4 \times \mathbb{R}$ and Ψ are bounded domains in \mathbb{R}_+^4 . Human mobility is considered in one-dimensional space i.e., $\nabla^2 = \partial^2 \partial x^2$. The result can be extended in higher-dimensional space, such as 2-dimensional space.

3. Well-Posedness of the Model

To ensure that the solutions of the model reflect the biological reality, the fundamental question of positivity and boundedness of the solutions is addressed in this section. The model is analyzed with zero flux boundary conditions (no movement across the boundary of $\partial\Psi$).

$$\frac{\partial S}{\partial n} = \frac{\partial E}{\partial n} = \frac{\partial I}{\partial n} = \frac{\partial R}{\partial n}, \quad (6)$$

where $((\partial)/(\partial n))$, denotes the outward normal derivative on $\partial\Psi$. Let the initial conditions be given by

$$\begin{aligned} S(x, t) = S(x, 0) \geq 0, E(x, t) = E(x, 0) \geq 0, I(x, t) = I(x, 0) \geq 0, \\ R(x, t) = R(x, 0) \geq 0. \end{aligned} \quad (7)$$

For $x \in (-\infty, +\infty)$, Ψ is a bounded domain in \mathbb{R}_+^4 with smooth boundary $\partial\Psi$, and $t \geq 0$.

Proposition 1. *Suppose that the initial condition (7) holds, then the solutions of model (5) are nonnegative in $[0, +\infty)$ for all $t \geq 0$.*

Proof. Model (5) can be written as an abstract Banach space $X = \bar{C}(\Psi) \times C(\bar{\Psi})$ in the form

$$\begin{aligned} u' &= Au(t) + F(u(t)), \quad t > 0 \\ u(0) &= u^0 \in X, \end{aligned} \quad (8)$$

where $u = (S, E, I, R)^T$, $u(0) = (S(x, 0), E(x, 0), I(x, 0), R(x, 0))^T$, $Au(t) = (d_1 S, d_2 E, d_3 I, d_4 R)^T$, and

$$F(u(t)) = \begin{pmatrix} \Lambda - \frac{\beta SI}{1 + \eta I} - \mu S \\ \frac{\beta SI}{1 + \eta I} - (\mu + \varepsilon)E \\ \varepsilon E - (\mu + \lambda + \delta)I \\ \lambda I - \mu R \end{pmatrix}. \tag{9}$$

Clearly, F is locally Lipschitz in X , hence model (5) has local solutions on the interval $[0, T_{\max})$, where T_{\max} is the minimum existence time for the solutions of model (5) [16].

Model (5) can also be written in the following form:

$$\begin{aligned} \frac{dS}{dt} - d_1 \nabla^2 S &= F_1(S, E, I, R) \\ \frac{dE}{dt} - d_2 \nabla^2 E &= F_2(S, E, I, R) \\ \frac{dI}{dt} - d_3 \nabla^2 I &= F_3(S, E, I, R) \\ \frac{dR}{dt} - d_4 \nabla^2 R &= F_4(S, E, I, R). \end{aligned} \tag{10}$$

The functions $F_i(S, E, I, R)$ and $i = \{1, 2, 3, 4, 5\}$ are continuously differentiable and they satisfy the following conditions: $F_1(0, E, I, R) = \Lambda \geq 0$, $F_2(S, 0, I, R) = 0 \geq 0$, $F_3(S, E, 0, R) = 0 \geq 0$, $F_4(S, E, I, 0) = 0 \geq 0$, for all $\{S, E, I, R\} \geq 0$. Since $(S, E, I, R) \geq 0$ with positive initial conditions, then solutions of model (5) are positive. This completes the proof. \square

Proposition 2. *The solutions of model (5) are bounded in the region $\Psi \times T$ for all $t \geq 0$.*

Proof. To check for the boundedness, adding all the equations in model (5) and setting $D = \max \{d_1, d_2, d_3, d_4\}$ to obtain

$$\frac{\partial N(x, t)}{\partial t} \leq \Lambda - \mu N + D \nabla^2 N. \tag{11}$$

The inequality (11) has a unique solution of the form

$$\frac{\partial N(x, t)}{\partial t} \leq \Lambda - \int_{-\infty}^{\infty} \frac{\mu N}{\sqrt{4D\pi t}} e^{(-x^2)/4Dt} dx, \tag{12}$$

where the fundamental solution of inequality (12) is given by

$$K(t, x) = \begin{cases} \frac{1}{\sqrt{4D\pi t}} e^{(-x^2)/4Dt}, & x \in \mathbb{R} \quad t > 0, \\ 0, & x \in \mathbb{R} \quad t < 0. \end{cases} \tag{13}$$

For one-dimensional reaction-diffusion equation, equation (13) satisfies the following

$$K(t, x) = \int_{-\infty}^{+\infty} \frac{1}{\sqrt{4D\pi t}} e^{(-x^2)/4Dt} dx = 1. \tag{14}$$

Hence

$$\frac{dN}{dt} \leq \Lambda - \mu N. \tag{15}$$

Since $N(t, x) > 0$, solving this inequality (15) and taking the limit as $t \rightarrow \infty$. Hence by variation of constants formula, yields

$$\limsup_{t \rightarrow \infty} N(t, x) \leq \frac{\Lambda}{\mu} \tag{16}$$

Hence $N(t, x)$ is bounded. \square

From Proposition 1 and Proposition 2, it is clear that solutions of model (5) are positive and bounded for $t \geq 0$. Therefore, model (5) is mathematically and epidemiologically meaningful and it is now sufficient to consider its solutions in $\Psi \times T$.

4. Existence of Equilibrium Points

The disease-free equilibrium point is the state at which there is no infection spreading in the population.

Proposition 3. *Model (5) has a disease-free equilibrium denoted by $E_0 = \{(\Lambda/\mu), 0, 0, 0\}$ where $S = (\Lambda/\mu)$, and $E = I = R = 0$.*

The endemic equilibrium is the state at which the disease remains persistent in a given population.

Proposition 4. *The endemic equilibrium E_* of the (5) exists whenever $I^* > 0$ for $R_0 > 1$ and is given by $E_* = \{S^*, E^*, I^*, R^*\}$*

Proof. . Setting $d_i = 0$ for $i = \{1, 2, 3, 4\}$ in model (5), then from first equation of model (5) becomes

$$S^* = \frac{\Lambda \beta (1 + \eta I^*)}{\beta I^* + \mu (1 + \eta I^*)}. \tag{17}$$

Substituting equation (17) into second equation of model (5) yields

$$E^* = \frac{\beta \Lambda I^*}{(\mu + \varepsilon)(\beta I^* + \mu(1 + \eta I^*))}. \tag{18}$$

Now substituting equation (18) into the third equation of model (5) yields

$$I^* = \frac{\mu(R_0 - 1)}{(\beta + \mu\eta)}. \tag{19}$$

It is clear from equation (19) that $I^* > 0$ when $R_0 > 1$. This implies that there exists an endemic equilibrium for model (5) whenever $R_0 > 1$. \square

TABLE 1: The descriptive summary of the model parameters.

Parameter	Description	Unit/value units	Source
Λ	Recruitment rate	$3.178 \times 10^{-5} \text{ day}^{-1}$	[17]
μ	Natural death rate	$3.91 \times 10^{-5} \text{ day}^{-1}$	[17]
δ	Disease mortality rate	$1.03 \times 10^{-6} \text{ day}^{-1}$	[17]
λ	Human recovery rate	0.125 day^{-1}	[5]
β	Transmission probability	0.02 day^{-1}	Estimated
ε	Transition from E to I	0.0877 day^{-1}	[18]
η	Human saturation constant	0.05	Estimated
d_1	Susceptible diffusivity constant	(0-1.0) km day ⁻¹	Variable
d_2	Exposed diffusivity constant	(0-1.0) km day ⁻¹	Variable
d_3	Infected diffusivity constant	(0-1.0) km day ⁻¹	Variable
d_4	Recovered diffusivity constant	(0-1.0) km day ⁻¹	Variable

Evaluating matrix (28) at the Disease-free equilibrium $E^0 = ((\Lambda/\mu), 0, 0, 0, 0)$ yields

$$J_{E^0} = \begin{bmatrix} -\frac{\nu}{d_1 k} & \frac{\mu}{d_1 k^2} & 0 & 0 & 0 & \frac{\beta \Lambda}{\mu d_1 k^2} & 0 & 0 \\ 1 & 0 & 0 & 0 & 0 & 0 & 0 & 0 \\ 0 & 0 & -\frac{\nu}{d_2 k} & \frac{(\mu + \varepsilon)}{d_2 k^2} & 0 & -\frac{\beta \Lambda}{\mu d_2 k^2} & 0 & 0 \\ 0 & 0 & 1 & 0 & 0 & 0 & 0 & 0 \\ 0 & 0 & 0 & \frac{\varepsilon}{d_3 k} & -\frac{\nu}{d_3} & \frac{(\mu + \lambda + \delta)}{d_3 k^2} & 0 & 0 \\ 0 & 0 & 0 & 0 & 1 & 0 & 0 & 0 \\ 0 & 0 & 0 & 0 & 0 & \frac{\lambda}{d_4 k^2} & -\frac{\nu}{d_4 k} & \frac{\mu}{d_4 k^2} \\ 0 & 0 & 0 & 0 & 0 & 0 & 1 & 0 \end{bmatrix}. \tag{28}$$

The eigenvalues of the Jacobian matrix (28) evaluated at the disease-free equilibrium, ξ_1, \dots, ξ_8 are

$$\begin{aligned} \xi_{1,2} &= \frac{-\nu \pm \sqrt{\nu^2 + 4\mu d_1}}{2d_1 k} & \xi_{3,4} &= \frac{-\nu \pm \sqrt{\nu^2 + 4(\mu + \varepsilon)d_2}}{2d_2 k}, \\ \xi_{5,6} &= \frac{-\nu \pm \sqrt{\nu^2 + 4(\mu + \lambda + \delta)d_3}}{2d_3 k} & \xi_{7,8} &= \frac{-\nu \pm \sqrt{\nu^2 + 4\mu d_4}}{2d_4 k}. \end{aligned} \tag{29}$$

Clearly, ξ_1, \dots, ξ_8 are real-valued eigenvalues, since all the parameters of the model are positive. Therefore, a traveling wave profile, that travels at a speed $\nu > 0$, exists that connects the disease-free and endemic equilibrium states. This

means that if infectious individuals diffuse into a susceptible population, a transition zone of infection will form.

6. Numerical Simulations and Discussion

Simulation analysis of model (5) is presented to graphically illustrate the behaviour of the solutions of the model with varying rates of diffusivity. For purposes of simulation the parameter values are stated in Table 1 and unless otherwise stated the initial populations are taken to be $S(0, x) = 3000$, $E(0, x) = 2000$, $I(0, x) = 1500$, and $R(0, x) = 1000$.

Figures 1(a) and 1(b) show the simulations of the susceptible humans for varying values of diffusivity rate d_1 at 0.1 and 0.9, respectively. The number of the susceptible humans reduces faster when diffusivity rate is high and also reduces with an increase in space. When $d_1 = 0.9$, it would

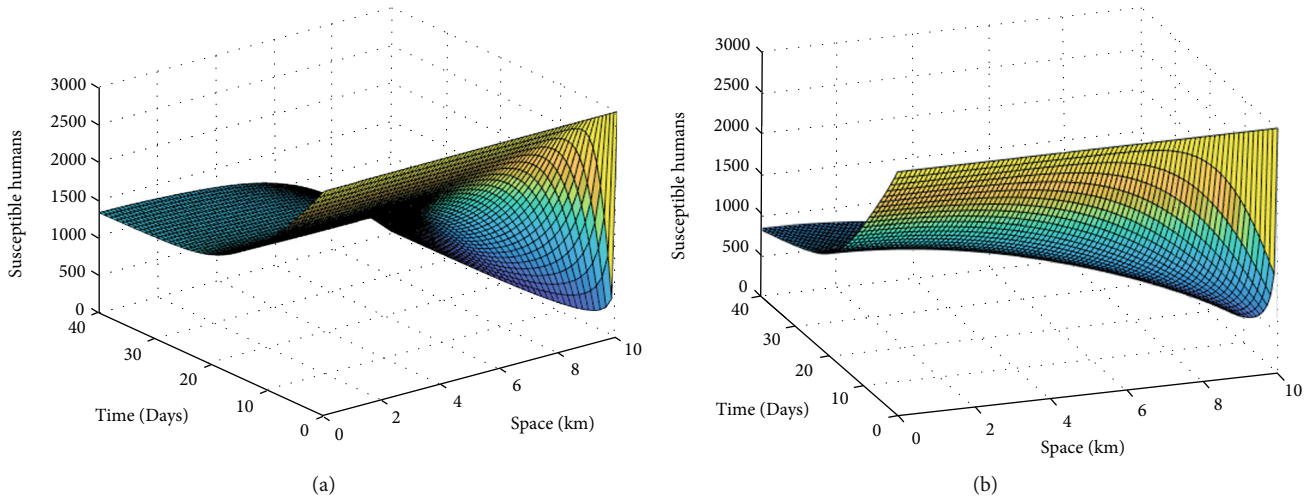


FIGURE 1: Plots (a) and (b) show the simulations of the susceptible humans corresponding to rate of diffusion, (a) $d_1 = 0.1 \text{ km day}^{-1}$, and (b) $d_1 = 0.9 \text{ km day}^{-1}$.

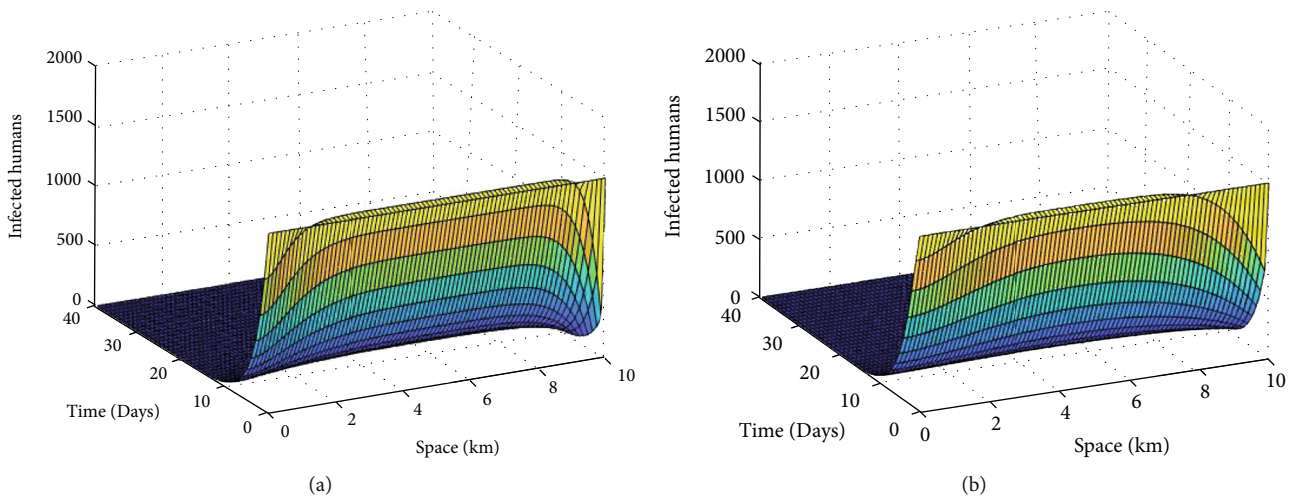


FIGURE 2: Plots (a) and (b) show the simulations of the Infected humans corresponding to the rate of diffusion, (a) $d_3 = 0.1 \text{ km day}^{-1}$, and (b) $d_3 = 0.9 \text{ km day}^{-1}$.

take less than 10 days for a pool of susceptible humans to be exposed to the virus. When diffusivity rate is low, $d_1 = 0.1$, it would take about 20 days for a pool of susceptible humans to become exposed once they come into contact with the virus.

Figure 2(a) and 2(b) show the spatiotemporal simulations of the infected humans for varying values of diffusivity rate d_3 . They show that as the rate of diffusion (human mobility), d_3 increases the number of infected individuals increases. This means that, human mobility has an effect in the transmission dynamics of COVID-19. Therefore, use of control interventions such as lock-down, travel restrictions, and cessation of movement that reduce human mobility may play a significant role in reducing COVID-19 spread. Infectious individuals will spread the infection to noninfected areas until an equilibrium is reached. The numerical results show that the disease persists in the population due to the movement of infectious individuals. The formation

of a wave profile indicates that the introduction of an infective individual into a susceptible population results in infection propagation.

7. Conclusion

The effect of human mobility on COVID-19 dynamics is investigated in this paper using a nonlinear parabolic partial differential equation. Well-posedness of the model and existence of steady states are shown. Existence of traveling wave solutions of the model are shown. The model analysis revealed that when infected individuals are introduced into a fully susceptible population, there is a moving transition “a propagating wave” of infections that connects the disease-free equilibrium to the endemic equilibrium. These waves propagate at speed $v > 0$, which connects the two equilibria points. From the numerical analysis, it is shown

that human mobility is critical for disease transmission. As a result, control interventions such as lock-down, travel restrictions, and cessation of movement that reduce human mobility may play a significant role in reducing COVID-19 spread. These interventions are aimed at creating barriers that will slow the spread of the virus in the affected areas.

Data Availability

All the data is within the text. However, the Matlab code used in simulation can be available on request

Conflicts of Interest

The authors declare that they have no conflicts of interest.

Acknowledgments

The authors would like to thank Masinde Muliro University of Science and Technology, Postgraduate Merit Scholarship Award for supporting this work.

References

- [1] V. Albani, J. Loria, E. Massad, and J. P. Zubelli, "The impact of COVID-19 vaccination delay: a sling study for Chicago and NYC data," 2021, <https://arxiv.org/abs/2102.12299>.
- [2] S. P. Adhikari, S. Meng, Y. J. Wu et al., "Epidemiology, causes, clinical manifestation and diagnosis, prevention and control of coronavirus disease (COVID-19) during the early outbreak period: a scoping review," *Infectious Diseases of Poverty*, vol. 9, no. 1, p. 29, 2020.
- [3] S. A. Lauer, K. H. Grantz, Q. Bi et al., "The incubation period of coronavirus disease 2019 (COVID-19) from publicly reported confirmed cases: estimation and application," *Annals of Internal Medicine*, vol. 172, no. 9, pp. 577–582, 2020.
- [4] Y. Mammeri, "A reaction-diffusion system to better comprehend the unlockdown: application of SEIR-type model with diffusion to the spatial spread of COVID-19 in France," *Computational and Mathematical Biophysics*, vol. 8, no. 1, pp. 102–113, 2020.
- [5] A. Aleta, D. Martin-Corral, A. Pastore et al., "Modelling the impact of testing, contact tracing and household quarantine on second waves of COVID-19," *Nature Human Behaviour*, vol. 4, no. 9, pp. 964–971, 2020.
- [6] M. Amaku, D. T. Covas, F. A. B. Coutinho, R. S. Azevedo, and E. Massad, "Modelling the impact of delaying vaccination against SARS-CoV-2 assuming unlimited vaccine supply," *Theoretical Biology and Medical Modelling*, vol. 18, no. 1, p. 14, 2021.
- [7] L. Azevedo, M. J. Pereira, M. Ribeiro, and A. Soares, *Spatio-temporal Modelling of COVID-19 Infection Risk in Portugal*, Research Square, 2020.
- [8] R. M. Anderson and R. M. May, *Infectious Disease of Human: Dynamics and Control*, Oxford University Press, UK, London, 1991.
- [9] H. W. Hethcote, "The mathematics of infectious diseases," *SIAM Review*, vol. 42, no. 4, pp. 599–653, 2000.
- [10] K. F. Tireito, G. O. Lawi, and C. A. Okaka, "HIV/AIDS treatment model with the incorporation of diffusion equations," *Applied Mathematical Sciences*, vol. 12, no. 12, pp. 603–615, 2018.
- [11] C. M. Wachira, G. O. Lawi, and J. Malinzi, "A spatiotemporal model on the transmission dynamics of Zika virus disease," *Asian Research Journal of Mathematics*, vol. 10, no. 4, pp. 1–15, 2018.
- [12] Y. Zhou, R. Xu, D. Hu, Y. Yue, Q. Li, and J. Xia, "Effects of human mobility restrictions on the spread of COVID-19 in Shenzhen, China: a modelling study using mobile phone data," *The Lancet Digital Health*, vol. 2, no. 8, pp. e417–e424, 2020.
- [13] M. Cevik, K. Kuppalli, J. Kindrachuk, and M. Peiris, "Virology, transmission, and pathogenesis of SARS-CoV-2," *bmj*, vol. 371, 2020.
- [14] J. G. Wagner, "Properties of the Michaelis-menten equation and its integrated form which are useful in pharmacokinetics," *Journal of Pharmacokinetics and Biopharmaceutics*, vol. 1, no. 2, pp. 103–121, 1973.
- [15] N. Ahmed, M. Fatima, D. Baleanu et al., "Numerical analysis of the susceptible exposed infected quarantined and vaccinated (SEIQV) reaction-diffusion epidemic model," *Frontiers in Physics*, vol. 7, p. 220, 2020.
- [16] L. El Mehdi, M. Mehdi, H. Khalid, and Y. Noura, "Partial differential equations of an epidemic model with spatial diffusion," *International Journal of Partial Differential Equations*, vol. 2014, Article ID 186437, 6 pages, 2014.
- [17] D. Martínez-Rodríguez, G. Gonzalez-Parra, and R. J. Villanueva, "Analysis of key factors of a SARS-CoV-2 vaccination program: a mathematical modeling approach," *Epidemiologia*, vol. 2, no. 2, pp. 140–161, 2021.
- [18] J. K. K. Asamoah, C. S. Bornaa, B. Seidu, and Z. Jin, "Mathematical analysis of the effects of controls on transmission dynamics of SARS-CoV-2," *Alexandria Engineering Journal*, vol. 59, no. 6, pp. 5069–5078, 2020.